A MULTIMODE GRAY-SCALE CMOS OPTICAL SENSOR FOR VISUAL COMPUTERS.

G. LIÑÁN, A. RODRÍGUEZ-VÁZQUEZ, S. ESPEJO, R. DOMÍNGUEZ-CASTRO, and E. ROCA

Instituto de Microelectrónica de Sevilla – CNM-CSIC
Edificio CICA-CNM, C/Tarfia s/n, 41012- Sevilla, SPAIN
Phone: +34 95 5056666, Fax: +34 95 5056686, E-mail: linan@imse.cnm.es[a]

This paper presents a new multimode optical sensor architecture for the optical interface of Visual CNN chips. The sensor offers to the user the possibility of choosing the photo-sensitive device as well as the mechanism for transducing the photogenerated charges into the correspondent pixel voltage. Both linear or logarithmic compression acquisition modes are available. This makes the sensor very suitable to be used in very different illumination conditions.

1 Introduction

CNNUMs [1] have demonstrated, theoretically in most of cases, their suitability for solving real-time image processing problems. The main advantage provided by its computing paradigm consists of completely executing the vision processing algorithm in a parallel way, which avoids the bottlenecks existing in conventional non-fully parallel solutions due to the need of serial data transferences between processors and memories. Nevertheless, if the images to be processed by the system must be electrically loaded to the CNN chips, as usually happens, a different bottleneck in data transmission may still exists. This problem relies on the fact that, for moderately large images -approx. 15x15- it is not possible to have a cell-per-I/O pin [b], and hence, data communications must be carried out in a serial manner. This is not only important because of the time required to transfer images to the CNN chip but also for the lack of a direct interaction between the CNN processor and the imager which avoids for the CNN chip to control, in some way, the characteristic of the visual acquisition process -integration time, characteristic of the sensing scheme, etc.

Those problems have been solved in some CNN chips -e. g. [2] - by adding a photosensor to each cell in the array. This makes the chip capable of capturing -in parallel- the visual information to be processed and even to control the characteristics of the sensing process. This solution also has the advantage of producing more compact vision systems since the camera, and the possible adapters between camera and chip, can be removed.

This paper presents a new multimode pixel architecture which can be easily incorporated to a standard CNN cell. The presented pixel has the capability of -by reconfiguration- acquire visual information in very different illumination conditions since it provides both, linear integration and logarithmic compression sensing schemes.

a. This work has been partially funded by ONR-NICOP N0014-00-C-0295 (POAC), DICTAM IST-1999-19007, and CICYT TIC 1999-0826.

b. It does not seem to be possible to have more than 225 I/O pins for data transmission.

2 Physical Foundations for Light Sensing in CMOS

Photodevices are the elements which allow for the combination of sensory and processing planes in a single chip. Several possibilities for the architecture of the photosensor exist, however, all of them rely on the same physical phenomenon, the photoelectric effect. Covalent bonds holding the electrons at their atomic sites in the lattice can be broken by an incident radiation if the energy of the incident photon is greater than the silicon band gap. Since this energy level is about 1.124eV, those photons with wavelengths below $1.1\mu\text{m}$ could be, theoretically, powerful enough to excite carriers from the valence band into the conduction one, thus producing the photogeneration.

Unfortunately, not all the photogenerated carriers are detected. Recombination phenomena make the number of created pairs to decrease very fast. Typical carrier life times in standard CMOS technologies are in the order of $0.1\mu\text{s}$ to $10\mu\text{s}$ and, therefore, efficient mechanisms to collect them before they recombine must be provided. The simplest method to do this consists of using reverse biased diodes. If photogeneration occurs within the depleted quasi-neutral region of the p-n junction, the built-in junction potential will quickly separate electrons and holes. These carriers form a current whose value can be quantified by the following expression [3],

$$I_{ph} = \frac{\eta \cdot q \cdot P_i}{h \cdot \upsilon} \tag{1}$$

where, η is the quantum efficiency, q is the electron charge, P_i is the density of power of the incident light, and $h \cdot \upsilon$ is the energy of one photon with frequency υ.

The quantum efficiency figure, η, expresses the quotient between the number of generated pairs and the number of incident photons with a certain frequency υ.

$$\eta(\upsilon) = \frac{\text{no. of detected charges}}{\text{no of incident photons}} \tag{2}$$

which is always lower than unity in the visible and infrared portion of the spectrum.

The number of charges photogenerated by an incident light with a power P_0 and a wavelength λ detected during a given time interval ΔT_{int} by using a photosensor of area A and a quantum efficiency $\eta(\lambda)$ is given by [5],

$$\Delta n = \frac{A \cdot P_0 \cdot \Delta T_{int}}{h \cdot c \cdot \lambda^{-1}} \cdot \eta(\lambda) = A \cdot P_0 \cdot H \cdot \xi(\lambda) \cdot \Delta T_{int} \tag{3}$$

where H is a physical constant defined as $H = (h \cdot c)^{-1}$ and $\xi(\lambda) \equiv \lambda \cdot \eta(\lambda)$ is a function of the wavelength of the incident light.

The total amount of electrical charge detected is simply obtained as,

$$Q_{ph} = q \cdot \Delta n = [A \cdot \xi(\lambda) \cdot \Delta T_{int}] \cdot P_0 \cdot q \cdot H \tag{4}$$

while the equivalent current produced within this interval is,

$$I_{ph} = Q_{ph} \times (\Delta T_{int})^{-1} = [A \cdot \xi(\lambda)] \cdot P_0 \cdot q \cdot H \tag{5}$$

Most usually, the photogenerated current is converted into an equivalent voltage value by using one of the following methods; the integration of the photogenerated current onto a previously initialized capacitor, or the transformation of the current into a voltage by

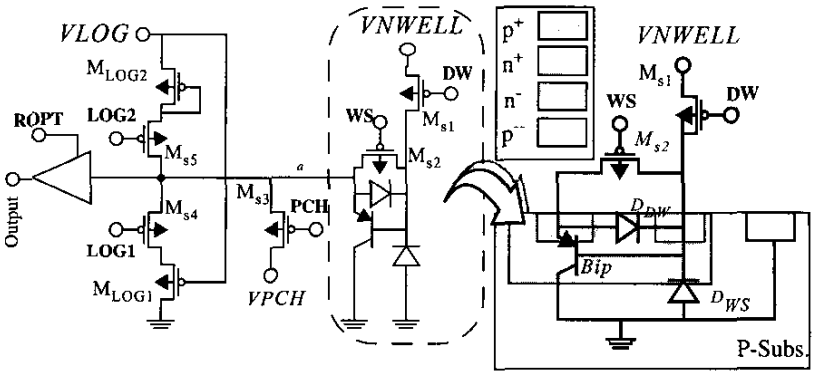

Figure 1. Representation of the Multimode Pixel. a) Schematic.

driving some kind of resistive load. In any case, attempts to linearly cover the huge range of illuminations existing in real life scenes[c] -6 to 8 decades- will always fail due to the fundamental limits imposed by noise floor and power supply level.

An interesting possibility to expand the sensor dynamic range -by renouncing to linearity- consists of using a non-linear I-V conversion block with a compressive characteristic. A suitable non-linear characteristic for visual signal compression is the logarithmic function. Its suitability comes from the evidence [6] that photoreceptors in the human retina exhibit a logarithmic-type response to light stimulus which provides a high dynamic range of operation.

We will see in the next sections how to exploit the photo-sensitive devices existing in standard CMOS technologies to obtain a multimode photosensor.

3 The Multimode Optical Sensor

3.1 Sensor Schematic

Fig. 1 shows the architecture of proposed sensor which can be divided into three blocks. The first one, a tri-state readout buffer, is used to control the communications among the sensor and others blocks in the CNNUM cell -basically the LAM module. Sensor readouts are controlled by the global programming signal **ROPT** -which corresponds to one bit in the Switch Configuration Register SCR.

The second part of the sensor is composed by the circuitry devoted to the transduction of the photo-generated charges into a voltage. The user has the possibility of selecting the phototransduction mechanism by means of SCR signals **LOG1, LOG2, PCH** as will be explained later.

The third block includes the optical sensor itself and two configuration switches $M_{s1,2}$ used to select one out of the three available photosensors. The selection of the sensor is carried out by other SCR programming signals **DW** and **WS**.

c. In humans, ~200dB separate the glare limit from the scotopic threshold.

3.2 *Integration Modes*

In integration modes, the sensor provides an output voltage which linearly depends on the intensity of the incident light. Independently of the actual photosensor selected, the sensing procedure is always the same. First of all, $M_{s5,4}$ are turned off by making **LOG1=LOG2**=1. Afterwards, switch M_{s3} precharges the internal node *a* to an user definable voltage *VPCH*. Finally, switch M_{s3} is turned off and the photogenerated current I_{ph} charges or discharges the pixel capacitor C_{pix}.

Fig. 2 shows the three different configurations for linear integration. Fig. 2 (a) shows the equivalent schematic for the first integration mode. It uses the N-Well/P-Subs photodiode (D_{WS}) as light sensitive device. The P-Diff/N-Well diode is annulled by making signal **WS**=0, while the bipolar transistor is also off by the same signal since it forces $V_{BE} = 0$. Then, it is easy to obtain that,

$$V_a = VPCH - \frac{I_{Ph}}{C_{pix}} T_{int} = VPCH - \frac{T_{int}}{C_{pix}} \times [A_{WS} \cdot \xi_{WS}(\lambda)] \cdot P_0 \cdot q \cdot H \qquad (6)$$

where A_{WS} is the sensing area of the N-Well/P-Subs photodiode, P_0 is the power of the incident light per area unit, and $\xi(\lambda) \equiv \lambda \cdot \eta_{WS}(\lambda)$.

Fig. 2 (b) shows the sensor schematic when the P-Diff/N-Well photodiode is used.By setting **WS**=1, **DW**=0 and *VNWELL* to the supply level, we ensure that the N-Well/P-Diff diode remains reverse biased, and that the vertical bipolar transistor is OFF. Only the carriers collected by the P-Diff/N-Well junction will contribute to the photocurrent yielding,

$$V_a = VPCH + \frac{I_{Ph}}{C_{pix}} T_{int} = VPCH + \frac{T_{int}}{C_{pix}} \times [A_{DW} \cdot \xi_{DW}(\lambda)] \cdot P_0 \cdot q \cdot H \qquad (7)$$

Finally, Fig. 2 (c) shows the schematic of the sensor when **WS=DW=1**. In this case, the base of the vertical BJT remains in open circuit. Photogenerated minority carriers in the base-emitter junction produce an emitter-base current which is amplified by the transistor effect. In this case, the output is simply given by

$$V_a = VPCH - \beta \times \frac{T_{int}}{C_{pix}} \times [A_{DW} \cdot \xi_{DW}(\lambda)] \cdot P_0 \cdot q \cdot H \qquad (8)$$

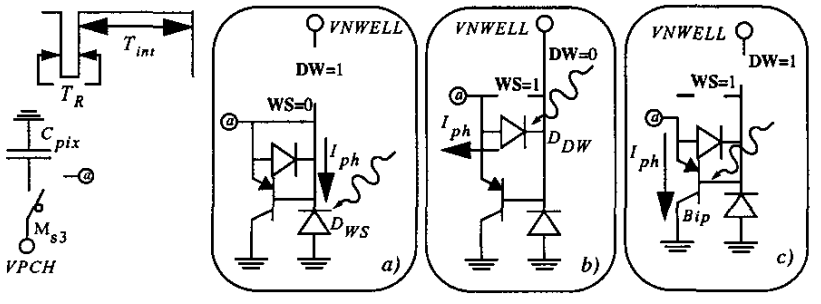

Figure 2. Available Configurations for Integration Modes.

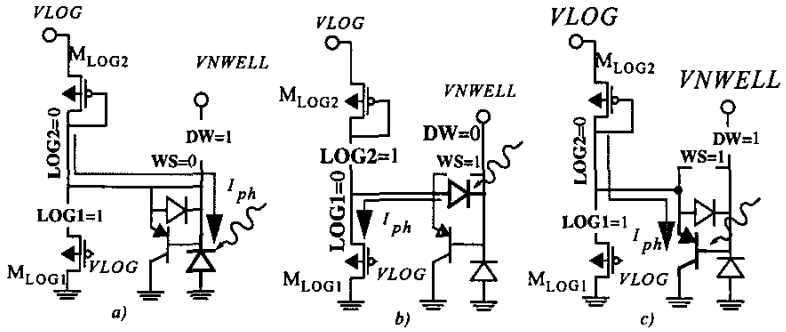

Figure 3. Available Configurations for Standard Log.Compression Modes.

Linear sensing schemes are limited to images where the existing dynamic range is relatively narrow. The next section shows how the proposed multimode sensor can be configured to perform different log-compression sensing schemes.

3.3 Logarithmic Compression with Transistor-based Loads

Logarithmic-type sensing has the advantage of producing images in which the difference between pixels only depends on the difference in optic contrast and not on global illumination conditions. Then, sensors exhibit a higher dynamic range DR. However, the price to be paid for that DR increase is a reduction of the contrast in the image -mostly due to the log function.

Most log-type reported image sensors exploit the logarithmic relationship existing between the current and the gate to source voltage when MOS transistors operate in the subthreshold regime. This property is used in our sensor as follows.

Fig. 3 shows the configurations available for this type of log-sensing in the proposed circuit. It can be seen that the reset transistor M_{s3} has been removed from the schematic since log-mode acquisitions work in continuous time -the output voltage corresponds to the equilibrium point of driving the non-linear resistive load with the photogenerated current. On the other hand, the selection of the active load must be properly done according to the sensor choice. Assuming that the drain to source current for a saturated PMOS transistor -bulk terminal connected to V_{dd} -within its subthreshold region is approximately given by[d] [7],

$$I_{DS} = I_{D0} \cdot e^{\left(\frac{n_p V_S - V_G - V_{T0} - (n_p - 1)V_{dd}}{n_p U_T}\right)} \tag{9}$$

it can be found that the steady state output voltages are given by,

d. The definition of the parameters in this expression can be found in [7].

$$V_a = n_{p_2} VLOG - V_{T0_{M2}} - \left(n_{p_{M2}} - 1\right) V_{dd} - n_{p_{M2}} U_T Ln\left[\frac{A_{WS} \cdot \xi_{WS}(\lambda) \cdot P_0 \cdot q \cdot H}{I_{D0_{M2}}}\right]$$

$$V_a = \frac{VLOG + V_{T0_{M1}} + \left(n_{p_{M1}} - 1\right) V_{dd} + n_{p_{M1}} U_T Ln\left[\frac{A_{DW} \cdot \xi_{DW}(\lambda) \cdot P_0 \cdot q \cdot H}{I_{D0_{M1}}}\right]}{n_{p_{M1}}} \tag{10}$$

$$V_a = n_{p_{M2}} VLOG - V_{T0_{M2}} - \left(n_{p_{M2}} - 1\right) V_{dd} - n_{p_{M2}} U_T Ln\left[\beta \frac{A_{DW} \cdot \xi_{DW}(\lambda) \cdot P_0 \cdot q \cdot H}{I_{D0_{M2}}}\right]$$

for circuits in Fig. 3 (a), (b), and (c), respectively.

In addition to the loss of contrast produced by the logarithmic function, it is also observed that the expressions for the output voltage contain several technological parameters related to the load transistor. Unfortunately, mismatching phenomena make those parameters to vary from pixel to pixel and, consequently, the Fixed Pattern Noise -FPN- figures in these kind of sensors are worst than that of their linear counterparts.

A possible alternative to solve this problem consists of using correlated-double sampling techniques [8] at the pixel level by exploiting the reconfiguration and algorithmic capabilities of the CNNUM cell. However, it may require adding new modules to the cell and the execution of a certain number of operations. In the next section we will present a log sensor which does not use any transistor load and that, consequently, exhibits better FPN figures.

3.4 Logarithmic Compression in the Photovoltaic Mode

The idea of using the photodiodes in the photovoltaic mode is relatively recent. It was first introduced and tested by Ni *et al.* in 1994 [9]. Experimental results demonstrate that this kind of sensors sensor exhibit a very high dynamic range and good uniformity FPN performances. The basic concept introduced by this sensing scheme consists of using a photodiode in an open circuit configuration, and to let it reach its steady state. In our case it works as follows.

Suppose the circuit in Fig. 1 (b). If no resistive load is connected to node a, and the circuit is allowed to achieve its steady state condition, the charge conservation principle imposes that the current flowing from *VNWELL* to node a -that is $I_S + I_{ph}$ [e]- must be equal to that flowing through the diode. Assuming that the diode is governed by the typical exponential equation, it yields,

$$V_a = VNWELL + nU_T Ln\left(\frac{I_{ph} + I_S}{I_S}\right) \tag{11}$$

which expresses a log-type relationship between the pixel output and the light intensity. The main advantage of this log-compression scheme is that the obtained expression is simpler -it involves only a few terms- than those on (10), and consequently, its operation is intrinsically more robust against cell-to-cell discrepancies.

e. I_S is the saturation current of the diode.

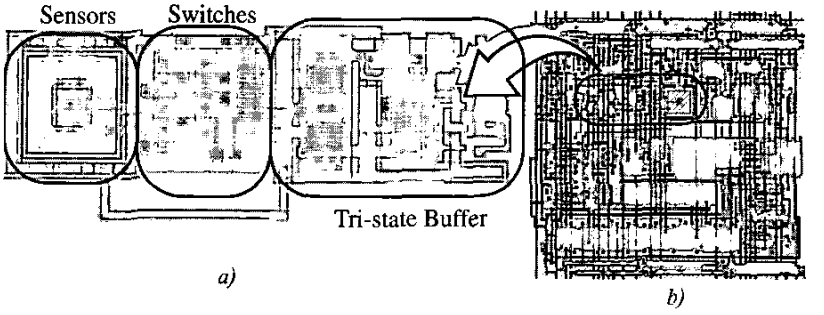

Figure 4. Layout Views. a) Sensor Layout. b) Cell Layout in ACE16K

3.5 Sensor Layout

The multimode sensor described in this paper has been included into the cell used by the ACE16K [10] prototype.

Fig. 4 (a) shows the layout of the sensor in the ACE16K chip. The N-Well in which the sensor is laid-out is $9.8\mu m \times 9.8\mu m$. A silicided protection mask has been also drawn all around the sensing area in order to avoid for the sensor to loss sensitivity. In addition, all the reconfiguration switches are PMOS type and laid-out in a different N-Well for isolation purposes. Finally, as can be seen in Fig. 4 (b), all the metal layers contain a hole on top of the sensor to avoid it to be covered.

4 Conclusions

We have presented a new multimode optical sensor architecture for the optical interface of Visual CNN chips. The sensor offers the possibility of selecting the actual light-sensitive device as well as the mechanism for transducing the photogenerated charges. Both linear and log compression acquisition modes are available, making the sensor very suitable to fit into very different illumination conditions.

References

1. T. Roska and L. O. Chua, "The CNN Universal Machine: An Analogic Array Computer". *IEEE Transactions on circuits and Systems-II: Analog and Digital Signal Processing*, Vol. 40, No. 3, pp. 163-173, March 1993.
2. R. Domínguez-Castro, S. Espejo, A. Rodríguez-Vázquez, R. Carmona, P. Foldesy, A. Zarándy, P. Szolgay, T. Sziranyi and T. Roska, "A 0.8 μm CMOS Programmable Mixed-Signal Focal-Plane Array Processor with On-Chip Binary Imaging and Instructions Storage", *IEEE Journal of Solid State Circuits*, Vol. 32, No. 7, pp. 1013-1026, July 1997.
3. R. W. Boyd, *Radiometry and the Detection of Optical Radiation*, Wiley-Interscience, 1983.

4. B. Saleh and M. Teich, *Fundamentals of Photonics*, John Wiley and Sons, Inc., New-York, 1991.

5. E. Roca *et al.*, "Chapter 5: Light Sensitive Devices in CMOS", in T. Roska and A. Rodríguez-Vázquez (Eds.), *Towards the Visual Microprocessor*, ISBN: 0-471-95606-6, John Wiley & Sons Ltd., Chichester, England, 2001.

6. T. Tomita, "Electrical Response of Single Photo Receptors", *Proc. of the IEEE, Special Issue on Neural Studies,* Vol. 56, pp. 1015-1023, 1968.

7. A. Rodríguez-Vázquez *et al.* "Chapter 3: CMOS Analog Design Primitives" in T. Roska and A. Rodríguez-Vázquez (Eds.), *Towards the Visual Microprocessor*, John Willey & Sons Ltd., Chichester, England, 2001, ISBN: 0-471-95606-6.

8. H. Wey and W. Guggenbuhl, "An Improved Correlated Double Sampling Circuit for Low Noise Charge-Coupled-Devices", *IEEE Trans. on Circuits and Systems*, Vol. 37, pp. 1559-1565, Dec. 1990.

9. Y. Ni, F. Lavainne and F. Devos, "CMOS Compatible Photoreceptor for High-Contrast Car Vision", *Intelligent Vehicle Highway systems, SPIE's International Symposium on Photonics for Industrial Applications,* Oct-Nov, 1994, Boston, pp. 246-252.

10. G. Liñán, A. Rodríguez-Vázquez, S. Espejo and R. Domínguez-Castro, "ACE16K: A 128x128 Focal Plane Analog Array Processor with Digital I/O", *Proc. of the CNNA 2002.*